We are IntechOpen, the world's leading publisher of Open Access books
Built by scientists, for scientists

6,900
Open access books available

186,000
International authors and editors

200M
Downloads

Our authors are among the

154
Countries delivered to

TOP 1%
most cited scientists

12.2%
Contributors from top 500 universities

CLARIVATE ANALYTICS
BOOK CITATION INDEX
INDEXED

WEB OF SCIENCE™

Selection of our books indexed in the Book Citation Index in Web of Science™ Core Collection (BKCI)

Interested in publishing with us?
Contact book.department@intechopen.com

Numbers displayed above are based on latest data collected.
For more information visit www.intechopen.com

2

Dynamically Improved 6-DOF System for Measurements of Forces and Torques in Wind Tunnels

V. Portman, B. Sandler and V. Chapsky
Ben Gurion University of the Negev, ISRAEL

1. Introduction

Investigation of bodies liable to high speed or variable airflows is a subject of importance. Determination of force and torque vectors acting on the latter is necessary to establish strength of the body and flow behavior. Airflow influence on a body (or system of bodies) is used in science and industry to define the values of air resistance parameters acting on this body. Resisting forces and torques, lifting or carrying forces and torques, and air attacking angles are examples of such types of parameters. This work deals 6-DOF force and torque measuring suited for use in air tunnels, comparing it with the existing methods used for the same purpose. Except for the body under investigation and its fastening elements nothing else is placed inside the tunnel. Six force sensors (load cells) and their fastening design is organized outside the air tunnel by means of a metal cubic (or other) frame were suspended on a massive base. Mathematical expressions describing the measurement and computation process of the values of the above mentioned 6 force and torque vectors are proposed. Examples of measuring processes and graphical presentations of some experimental results are given in this work. In this work we propose further development of the discussed design by reducing the mass and inertia moments of this frame and relative positioning the model to it, in such a way reducing the caused by these dynamic parameters disturbing the measurements. In this case the model pattern for air flow influence measurements were made on a flat disc-like body.

2. Brief overview of wind tunnels.

Means for studying and determining the forces and torques acting on bodies influenced by high air flow speeds or subjected to variable wind speeds in air tunnels are required for both science and industry. This airflows influence on a body (or a system of bodies) is used for estimation the air resistance acting on these bodies or body. In the authors work [1] is brought a brief list of three balances that are usually applied for measuring wind drag forces and torques, lifting or carrying forces and torques, "air attacking angle" are examples of such parameters.

Partly the described in the mentioned paper measuring lay-outs are illustrated by examples given in Ewalds paper [2] from 2000. Another type of internal six- component wind-tunnel

balance is that having three-dimensional mechanism, as described by Gorlin and Slezinger [3], 2000. A solutin alike to mentioned here belongs also to Corliss and Cole [4] 1998. In these cases a multi-component balances are placed in the tunnel being by means of elastic cables connected to corresponding elements of the measured pattern. This set disturbs the air flow in the tunnel to some extent.

The model can be via an enough elastic rod connected to the tail part of the investigated model and provided with differently oriented strain gauges gives the needed measured information describing the acting forces and torques. Pope and Harper [5] 1999 describe developed some calibration rigs fir internal strain gauge balances.

The closest to the proposed design is the model placed on a platform inside the tunnel. And the forces are measured with 6-DOF hexapod-like balances placed outside the tunnel.(See Nguen et al.[6], 1002 and Kerr et al [7],1989)

In this work, we propose to use a fourth orthogonal structure of a parallel robot directly in the chain of force and moment components, acting on the model, and computation. An *idea came* to shorten the process of investigation of the forces and moments acting on the model in the tunnel, which avoids the amount of unnecessary bodies in the tunnel and their *interference*. This proposed measurement method in the wind tunnel is close to the discussed earlier external 6-DOF to certain extent improved approach. Some ideas of this kind where discussed in the authors work Chapsky et al. [10], 2007, and the work [11] of Lui, S.A. and Tso, H. L., 2002. The main purpose of this paper is to propose and demonstrate experimentation with a wind tunnel structure including the model to be investigated, a measuring element combined with a computer. This system (shown in Fig.1.) uses the corresponding functions (or equations) for each of six force and moment components depending upon the air speed and the shape of the investigated model. This work is devoted to introduce a different measuring approach and shows its advantages offering the fourth kind of dealing with the problem. The fourth kind of balance proposed in this paper has once calibrated load cells and once written computation program for any fixed model used for investigation.

- only one rod is placed in the tunnel for fastening the investigation pattern;
- the balances and measuring sensors (load-cells) are located outside the tunnel supplying the needed information to the computer;
- values of the acting, due to the wind, forces and torques are automatically shown on the computer's screen;
- there are no interactions between the six measured and computed values as it often happens in other systems.

Later we show 7 pages with computed examples of all here mentioned types (even those which we are not able to realize for our tunnel).

3. Experimental arrangement

A general view of the wind tunnel built at the Mechanical Engineering Department of Ben Gurion University of the Negev, Israel is shown in Fig.1.

In Fig.2 a close view of the wind tunnel near the outer frames and the places for movable frame's suspension are given. Also the door for the pattern fastening and its orientation is seen here. Fig.3 shows the load-cells used in this design. It used for the measuring the value of the mechanical response to the wind forces. The maximum air speed in the tunnel is *40 m/sec*. Length of the tunnel is about *30 m.*

Fig. 1. Wind tunnel device in the aero-dynamic laboratory of BGU of the Negev, (general view).

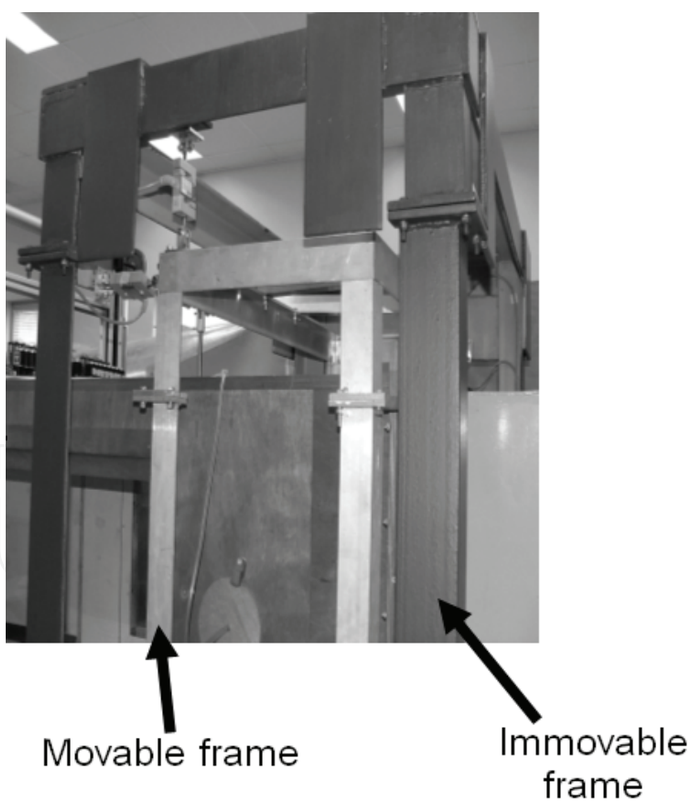

Fig. 2. Wind tunnel. The movable aluminum frame provides the information about the X, Y, and Z displacements of the pattern and its rotations around these axes. The steal made immovable frame is the base of the arrangement.

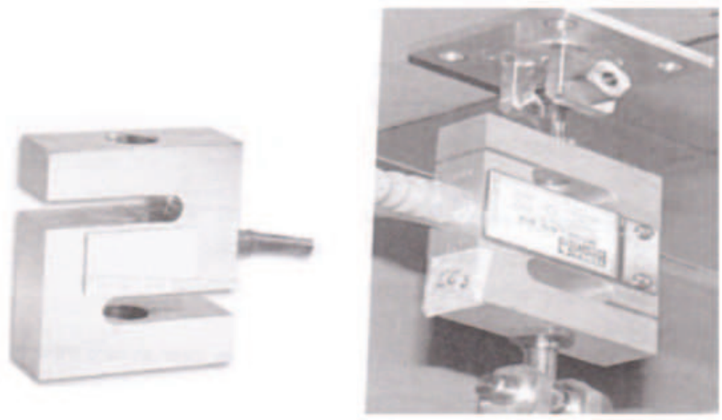

(a) (b)

Fig. 3. The Data-Logger of the 34970 type: (a) S-beam load cell, (b) view of the suspension including the Data-Logger.

Cross-section of the tunnel equals *0.7 x 0.7 m*². The pattern is fixed in the middle of the earlier mentioned rod as it is schematically shown in Fig.4. This experimental case discussed in work [1];

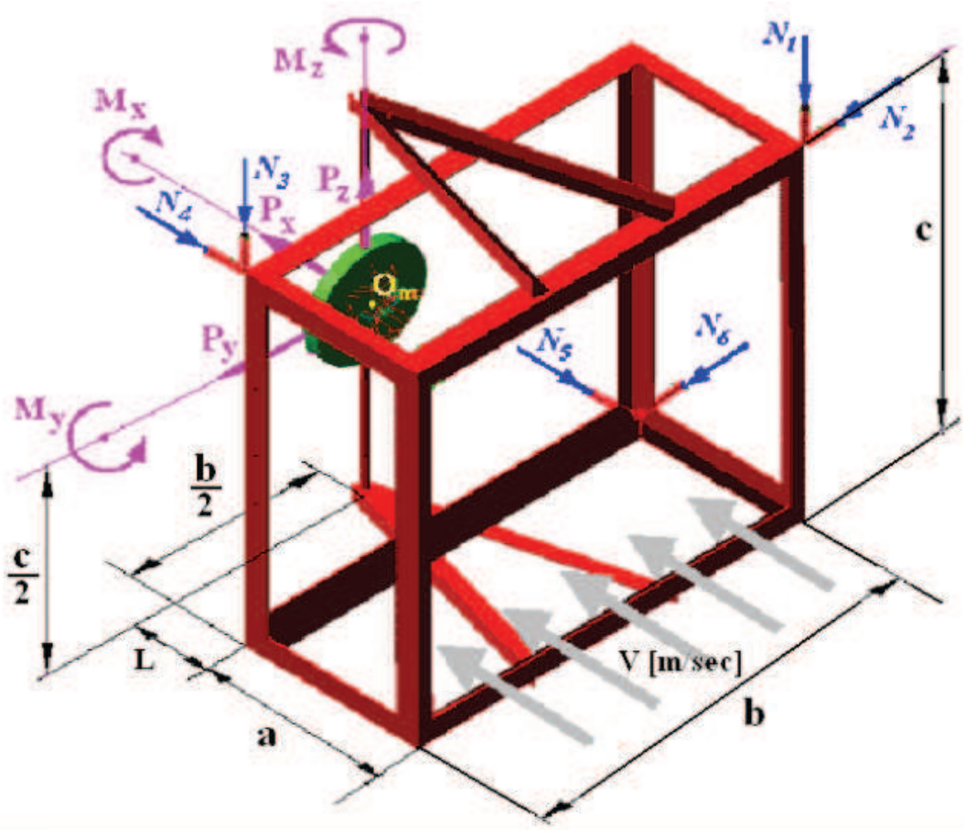

Fig. 4. Lay-out of the movable old frame primarily designed and built around the tunnel: a = 470, b = 1050, c = 1030, L = 200, (the dimensions are millimetres).

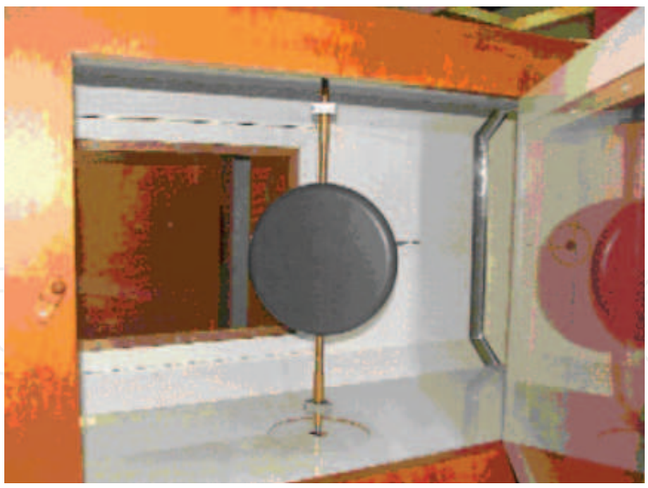

Fig. 5. Pattern location in the wind tunnel: flat disc placed in it.

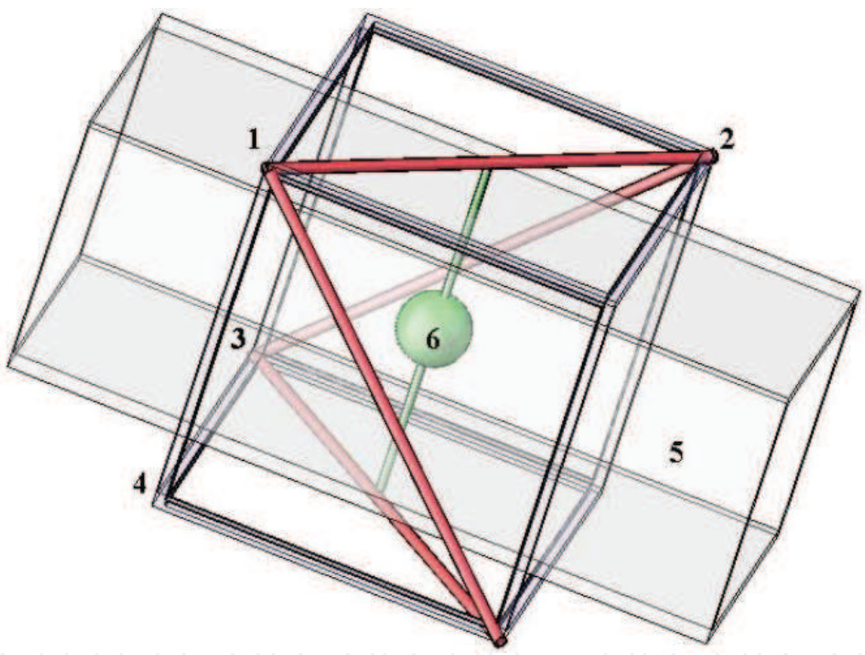

Fig. 6. Relative design of the new and old (previous) frame construction.

4. Main idea of the new frame design.

To improve the dynamical performance of the proposed apparatus the set of different frame arrangements has been investigated. The difference between experimental arrangements lies in the mass of the entire design, in the position of the tested pattern (flat disc) relative to the frame, and in the symmetry of the frame shape.

To reduce the mass of the frame without changing the geometric dimensions the new arrangement has been proposed. Its design is clear from figure 6. In the Fig.6 the red frame is the new proposed design, the "gray" profile 5 demonstrates the wind tunnel, the 'black" frame 4 is the previous design, 1, 2, 3 are the fastening points of the frame suspensions for both cases (new and old design), the green sphere 6 is the investigated pattern.

Every point of the frame suspensions has two directions of force measuring. For instance, the point 1 measures in directions "x" and "z", the point 2 measures in directions "z" and "y", point 3 in directions "x" and "y".
The investigated models were conventionally named as follows:
"Old" – with full set of 12 edges, "New" – with reduced mass (4 edges);
"Regular" – with pattern, located outside the frame;
"Central" – with pattern in the geometrical center of the frame;
"Symmetric" – with cube-shaped frame coverage figure.
The investigated frame designs and their dimensions are shown in Table 1.

Old Regular	New Regular	Old Central	New Central	Old symmetric	New Symmetric
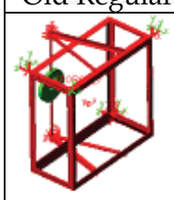	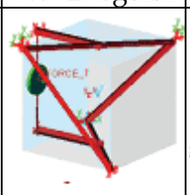	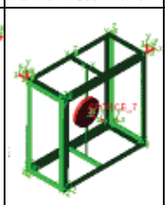	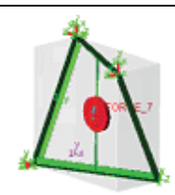	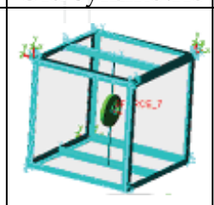	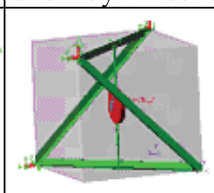
a = 470 b = 1050 c = 1030 L = 200	a = 1050 b = 1050 c = 1050 L = 200	a = 470 b = 1050 c = 1030 L = -a/2	a = 470 b = 1050 c = 1030 L = -a/2	a = 1050 b = 1050 c = 1050 L = -a/2	a = 1050 b = 1050 c = 1050 L = -a/2

Table 1. Proposed frames, their design and dimensions.

All these "Old" and "New" kinds of frames are checked dynamically and therefore can be accordingly analyzed.
The item we propose for publishing is somehow continuation of the paper published earlier and caused your attention. We speak about an improved design of the same principal structure, however improved because its main mass is considerably smaller despite the same geometric dimensions. The said is clear from the figure 6.

5. Dynamical investigation

Comparative dynamic investigations of virtual models of tunnel balances have been carried out by means of the interactive computer-based motion simulation software MSC ADAMS/View.
Every virtual model was loaded consequentially in all directions by harmonic forces or moments U(t) with varying frequency.

$$U(t) = U_0 \sin(\omega(t)*t) = U_0 \sin((1000*t)*t),$$

Where U_0 - initial magnitude of the force or moment, $\omega(t)$ –frequency, which depends on the time according equation: $\omega(t) = 1000*\text{time}$.
The responses of each spring have been measured and Bode plots were calculated with purpose to define the bandwidth of tested model. Bandwidth corresponds to the frequencies, where Bode-magnitude plot lay in the ±3dB range relative to the initial (steady-state) value. For convenience, the Bode plots were shifted to zero value in initial state by multiplying the measured results on some factors. All factors were calculated by symbolic mathematics software such as Mathematica-7. The applied Mathematica-7 program is shown in appendix 1.

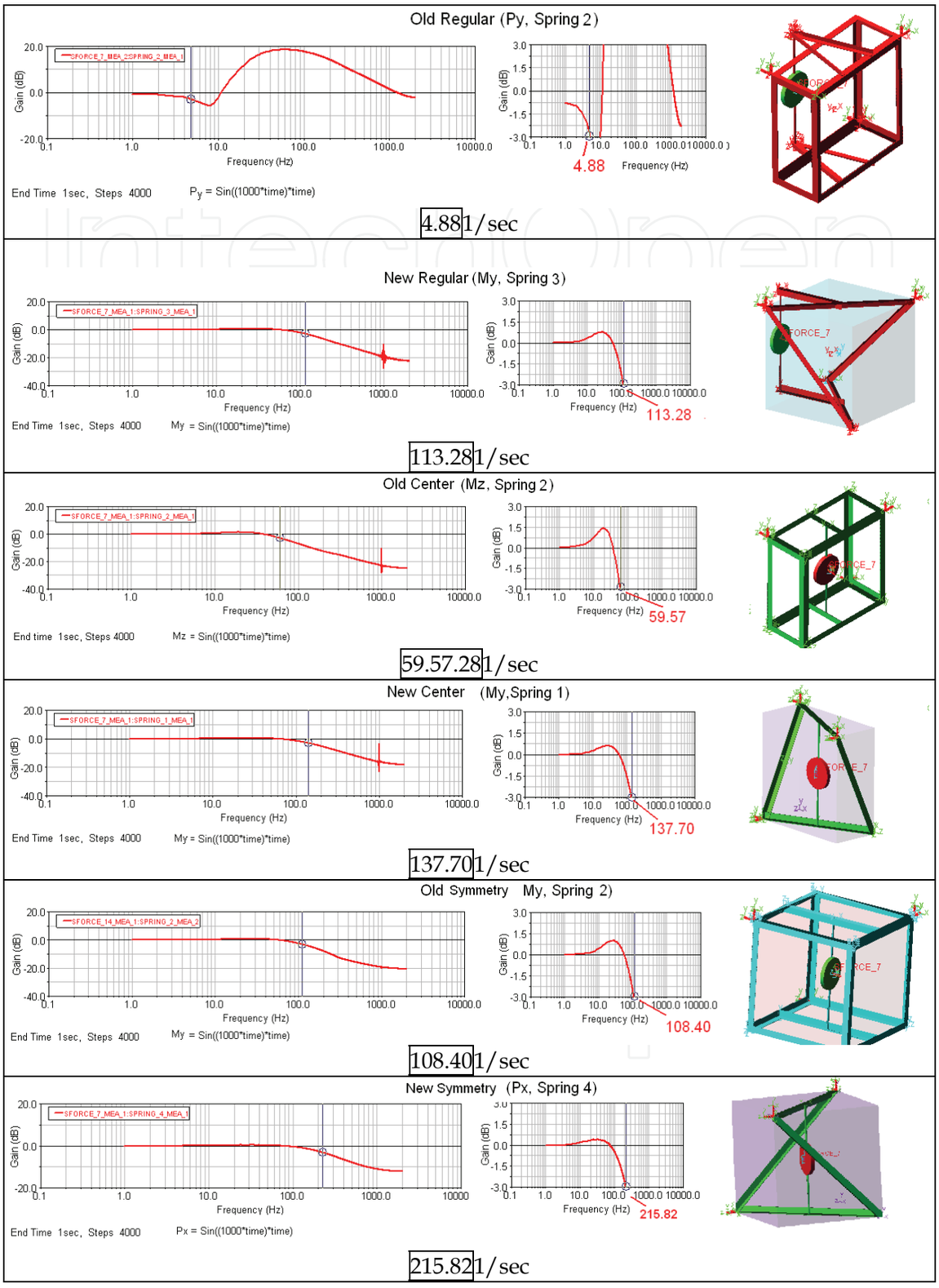

Table 2. The determinative Bandwidths

The worst Bode plots relative to spring forces and corresponding bandwidths for every force and torque directions (Px, Py, Pz, Mx, My, Mx, according notations in Figure 5) are shown in Appendix 2. The determinative ones for each design are shown in Table 2.
As clear from Table 2, the most desirable is the design "New Symmetry", which has bandwidth 215.82 Hz. The "New central" is applicable too. If it is not possible to locate the pattern in the center of the frame due to the limitations of the wind tunnel design the "New regular" model can be applied, but with bandwidth 113.28 Hz. All these models are better than earlier model "Old Regular", which has bandwidth 4.88Hz in Py and Pz directions, despite the fact that in Px direction it has bandwidth 156.25Hz.

6. Conclusions

1. The proposed device requires a universal sequence and simple action for receiving the measured data. Investigator must only fasten the pattern on the mentioned rod.
2. Dynamic estimations of the virtual model of proposed tunnel balance by means of the interactive computer-based ADAMS/View system showed that the working frequency of the proposed method and device are limited to a ~100÷200 Hz bandwidth.
3. The translational isotropy of the proposed device is defined by the independence of the sensitivity of measurement from the direction of the operating forces.
4. For estimation of the anisotropy of devices, the anisotropy index which equals to the ratio of maximum and minimum stiffness values is applied. Two types of indexes are separately used: for translational and rotational stiffness values (see Table 2).
5. The proposed devices "New Symmetry" and "Old Symmetry" has better dynamic features than conventionally used systems: it is fully isotropic from the point of view of translational stiffness and has a high level of isotropy from the view point of rotational stiffness.
6. The proposed device shows at least the theoretical possibility to improve the dynamic properties of the wind tunnel comparing with the already offered.

7. References

[1] V. Portman, B.Z. Sandler, V. Chapsky, I. Zilberman, A 6-DOF isotropic measuring system for force and torque components of drag for use in wind tunnels, (Innovative design), Int J Mech Mater Des (2009) 5:337-352.
[2] F R Ewald, Multi-component force balances for conventional and cryogenic wind tunnels, Meas. Sci. Technol.11 (2000) R81-R94. Conference, 20th, Albuquerque, NM, June 15-18, 1998
[3] S.M.Gorlin, I.I. Slezinger, Wind tunnels and their instrumentation, translated from Russian for NASA tt f-346, 2000.
[4] Alan Pope, Judu J. Harpes, Law speed wind tunnels testing, John Wiley & Sons, 1999.
[5] A. Bentur, N. S. Berke, Sidney Diamond -... Steel Corrosion in Concrete: Fundamentals and Civil Engineering Practice Arnon Israel Sidney Diamond School of Civil Engineering, Purdue University,1997, 201 pp.
[6] Tuttle, S.L., Mee, D.J., Simmons, J.M., Daniel W.J., et al., "NASA technical reports", 1994.
[7] S.R. Sanderson and J.M. Simmons, "Force Measurement in Impulse Facilities, Department of Mechanical Engineering ", University of Queensland, 2006
[8] C.C. Nguen, S.S. Antrazi, Z.-L.Zhou, C.E. Cambell, Jr. "Analysis and Experimentation of a Stewart Platform-based Force/Torque Sensor", International Journal of Robotics and Automation, Vol. 7, No. 3, 1992, 133 – 141.

[9] D.R. Kerr, "Analysis, Properties, and Design of a Stewart-Platform Transducer", in Transaction of the ASME, Journal of Mechanisms, Transmissions, and Automation in Design", March, 1989, Vol. 111/25, pp. 25 – 28.
[10] V. Chapsky, V. Portman, B-Z Sandler, 2007, Single-mass 6-DOF isotropic accelerometer with segmented PSD sensors, Sensors and Actuators: A physical, Vol. A135/2, pp. 558-569.
[11] Liu, S.A., Tso, H.L., 2002, A novel six-component force sensor of good measurement isotropy and sensitivities, Sensors and Actuators: A physical, Vol. A100, pp. 223-230.
[12] Z. Aliyazicioglu, Electrical and Computer Engineering Department, Cal Poly Pomona *ECE307-8*, ECE

Appendix 1. Mathematica-7 computation program.

```
"Removing all data";
Remove["Global`*"];
```

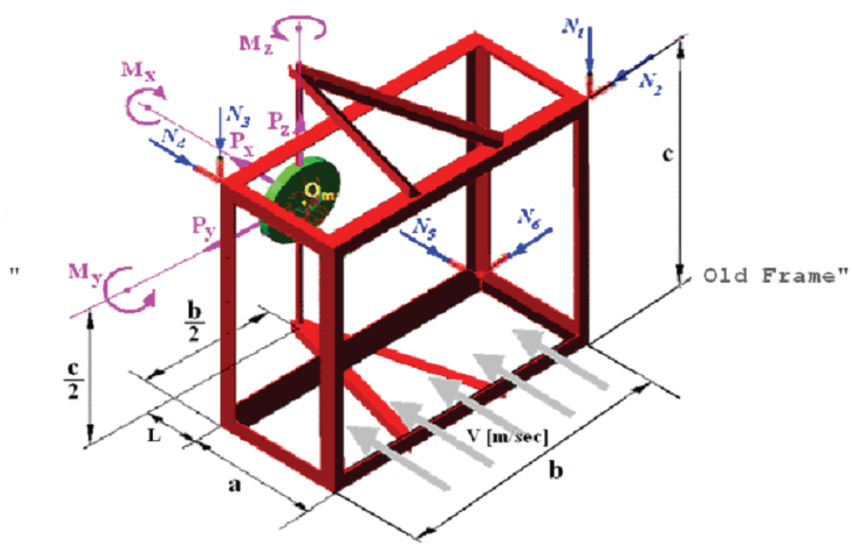


```
"Set of equations of static equilibrium of forces and moments"

M1 = {Px + N4 + N5 == 0, Py + N2 + N6 == 0, Pz + N1 + N3 == 0,
    Mx + N3 * b / 2 - N1 * b / 2 - N2 * c / 2 + N6 * c / 2 == 0,
    My + N3 * L + N1 * (L + a) - N5 * c / 2 + N4 * c / 2 == 0,
    Mz + N5 * b / 2 - N4 * b / 2 - N6 * L - N2 * (L + a) == 0};
MatrixForm[%]
```

$$\begin{pmatrix} N4 + N5 + Px == 0 \\ N2 + N6 + Py == 0 \\ N1 + N3 + Pz == 0 \\ -\frac{b\,N1}{2} - \frac{c\,N2}{2} + \frac{b\,N3}{2} + \frac{c\,N6}{2} + Mx == 0 \\ \frac{c\,N4}{2} - \frac{c\,N5}{2} + N3\,L + N1\,(a + L) + My == 0 \\ -\frac{b\,N4}{2} + \frac{b\,N5}{2} - N6\,L - N2\,(a + L) + Mz == 0 \end{pmatrix}$$

```
"Solving the system of equations"

SolvMatrix = Solve[M1, {N1, N2, N3, N4, N5, N6}]
```

$$\left\{\left\{N3 \to -\frac{2\,a\,Mx - 2\,b\,My - 2\,c\,Mz - a\,c\,Py - 2\,c\,L\,Py + 3\,a\,b\,Pz + 2\,b\,L\,Pz}{4\,a\,b},\right.\right.$$
$$N1 \to -\frac{-2\,a\,Mx + 2\,b\,My + 2\,c\,Mz + a\,c\,Py + 2\,c\,L\,Py + a\,b\,Pz - 2\,b\,L\,Pz}{4\,a\,b},$$
$$N4 \to -\frac{2\,a\,Mx + 2\,b\,My - 2\,c\,Mz + 2\,b\,c\,Px - a\,c\,Py - 2\,c\,L\,Py - a\,b\,Pz - 2\,b\,L\,Pz}{4\,b\,c},$$
$$N5 \to -\frac{-2\,a\,Mx - 2\,b\,My + 2\,c\,Mz + 2\,b\,c\,Px + a\,c\,Py + 2\,c\,L\,Py + a\,b\,Pz + 2\,b\,L\,Pz}{4\,b\,c},$$
$$N2 \to -\frac{-2\,a\,Mx - 2\,b\,My - 2\,c\,Mz + a\,c\,Py - 2\,c\,L\,Py + a\,b\,Pz + 2\,b\,L\,Pz}{4\,a\,c},$$
$$\left.\left.N6 \to -\frac{2\,a\,Mx + 2\,b\,My + 2\,c\,Mz + 3\,a\,c\,Py + 2\,c\,L\,Py - a\,b\,Pz - 2\,b\,L\,Pz}{4\,a\,c}\right\}\right\}$$

```
"Conditions of the simulation";

condPx = {Py -> 0, Pz -> 0, Mx -> 0, My -> 0, Mz -> 0};
condPy = {Px -> 0, Pz -> 0, Mx -> 0, My -> 0, Mz -> 0};
condPz = {Py -> 0, Px -> 0, Mx -> 0, My -> 0, Mz -> 0};
condMx = {Py -> 0, Pz -> 0, Px -> 0, My -> 0, Mz -> 0};
condMy = {Py -> 0, Pz -> 0, Mx -> 0, Px -> 0, Mz -> 0};
condMz = {Py -> 0, Pz -> 0, Mx -> 0, My -> 0, Px -> 0};


"Geometric conditions; Regular, Central, Symmetric,
   and L for central and symmetric configurations";

condGeomReg = {a -> 470, b -> 1050, c -> 1030, L -> 200};
condGeomSym = {a -> 1050, b -> 1050, c -> 1050};
condGeomCentr = {a -> 470, b -> 1050, c -> 1030};
condL = {L -> -a / 2};
```

```
"Numerical results";
```

```
RegPx = SolvMatrix /. condPx /. condGeomReg
```

$$\left\{\left\{N3 \to 0,\ N1 \to 0,\ N4 \to -\frac{Px}{2},\ N5 \to -\frac{Px}{2},\ N2 \to 0,\ N6 \to 0\right\}\right\}$$

```
RegPy = SolvMatrix /. condPy /. condGeomReg
```

$$\left\{\left\{N3 \to \frac{2987\,Py}{6580},\ N1 \to -\frac{2987\,Py}{6580},\ N4 \to \frac{29\,Py}{140},\ N5 \to -\frac{29\,Py}{140},\ N2 \to -\frac{7\,Py}{188},\ N6 \to -\frac{181\,Py}{188}\right\}\right\}$$

```
RegPz = SolvMatrix /. condPz /. condGeomReg
```

$$\left\{\left\{N3 \to -\frac{181\,Pz}{188},\ N1 \to -\frac{7\,Pz}{188},\ N4 \to \frac{87\,Pz}{412},\ N5 \to -\frac{87\,Pz}{412},\ N2 \to -\frac{9135\,Pz}{19\,364},\ N6 \to \frac{9135\,Pz}{19\,364}\right\}\right\}$$

```
RegMx = SolvMatrix /. condMx /. condGeomReg
```

$$\left\{\left\{N3 \to -\frac{Mx}{2100},\ N1 \to \frac{Mx}{2100},\ N4 \to -\frac{47\,Mx}{216\,300},\ N5 \to \frac{47\,Mx}{216\,300},\ N2 \to \frac{Mx}{2060},\ N6 \to -\frac{Mx}{2060}\right\}\right\}$$

```
RegMy = SolvMatrix /. condMy /. condGeomReg
```

$$\left\{\left\{N3 \to \frac{My}{940},\ N1 \to -\frac{My}{940},\ N4 \to -\frac{My}{2060},\ N5 \to \frac{My}{2060},\ N2 \to \frac{21\,My}{19\,364},\ N6 \to -\frac{21\,My}{19\,364}\right\}\right\}$$

```
RegMz = SolvMatrix /. condMz /. condGeomReg
```

$$\left\{\left\{N3 \to \frac{103\,Mz}{98\,700},\ N1 \to -\frac{103\,Mz}{98\,700},\ N4 \to \frac{Mz}{2100},\ N5 \to -\frac{Mz}{2100},\ N2 \to \frac{Mz}{940},\ N6 \to -\frac{Mz}{940}\right\}\right\}$$

```
CentrPx = SolvMatrix /. condPx /. condL /. condGeomCentr
```

$$\left\{\left\{N3 \to 0,\ N1 \to 0,\ N4 \to -\frac{Px}{2},\ N5 \to -\frac{Px}{2},\ N2 \to 0,\ N6 \to 0\right\}\right\}$$

```
CentrPy = SolvMatrix /. condPy /. condL /. condGeomCentr
```

$$\left\{\left\{N3 \to 0,\ N1 \to 0,\ N4 \to 0,\ N5 \to 0,\ N2 \to -\frac{Py}{2},\ N6 \to -\frac{Py}{2}\right\}\right\}$$

```
CentrPz = SolvMatrix /. condPz /. condL /. condGeomCentr
```

$$\left\{\left\{N3 \to -\frac{Pz}{2},\ N1 \to -\frac{Pz}{2},\ N4 \to 0,\ N5 \to 0,\ N2 \to 0,\ N6 \to 0\right\}\right\}$$

```
CentrMx = SolvMatrix /. condMx /. condL /. condGeomCentr
```

$$\left\{\left\{N3 \to -\frac{Mx}{2100},\ N1 \to \frac{Mx}{2100},\ N4 \to -\frac{47\,Mx}{216\,300},\ N5 \to \frac{47\,Mx}{216\,300},\ N2 \to \frac{Mx}{2060},\ N6 \to -\frac{Mx}{2060}\right\}\right\}$$

```
CentrMy = SolvMatrix /. condMy /. condL /. condGeomCentr
```

$$\left\{\left\{N3 \to \frac{My}{940},\ N1 \to -\frac{My}{940},\ N4 \to -\frac{My}{2060},\ N5 \to \frac{My}{2060},\ N2 \to \frac{21\,My}{19\,364},\ N6 \to -\frac{21\,My}{19\,364}\right\}\right\}$$

```
CentrMz = SolvMatrix /. condMz /. condL /. condGeomCentr
```

$$\left\{\left\{N3 \to \frac{103\,Mz}{98\,700},\ N1 \to -\frac{103\,Mz}{98\,700},\ N4 \to \frac{Mz}{2100},\ N5 \to -\frac{Mz}{2100},\ N2 \to \frac{Mz}{940},\ N6 \to -\frac{Mz}{940}\right\}\right\}$$

```
SymPx = SolvMatrix /. condPx /. condL /. condGeomSym
```

$$\left\{\left\{N3 \to 0,\ N1 \to 0,\ N4 \to -\frac{Px}{2},\ N5 \to -\frac{Px}{2},\ N2 \to 0,\ N6 \to 0\right\}\right\}$$

```
SymPy = SolvMatrix /. condPy /. condL /. condGeomSym
```

$$\left\{\left\{N3 \to 0,\ N1 \to 0,\ N4 \to 0,\ N5 \to 0,\ N2 \to -\frac{Py}{2},\ N6 \to -\frac{Py}{2}\right\}\right\}$$

```
SymPz = SolvMatrix /. condPz /. condL /. condGeomSym
```

$$\left\{\left\{N3 \to -\frac{Pz}{2},\ N1 \to -\frac{Pz}{2},\ N4 \to 0,\ N5 \to 0,\ N2 \to 0,\ N6 \to 0\right\}\right\}$$

```
SymMx = SolvMatrix /. condMx /. condL /. condGeomSym
```

$$\left\{\left\{N3 \to -\frac{Mx}{2100},\ N1 \to \frac{Mx}{2100},\ N4 \to -\frac{Mx}{2100},\ N5 \to \frac{Mx}{2100},\ N2 \to \frac{Mx}{2100},\ N6 \to -\frac{Mx}{2100}\right\}\right\}$$

```
SymMy = SolvMatrix /. condMy /. condL /. condGeomSym
```

$$\left\{\left\{N3 \to \frac{My}{2100},\ N1 \to -\frac{My}{2100},\ N4 \to -\frac{My}{2100},\ N5 \to \frac{My}{2100},\ N2 \to \frac{My}{2100},\ N6 \to -\frac{My}{2100}\right\}\right\}$$

```
SymMz = SolvMatrix /. condMz /. condL /. condGeomSym
```

$$\left\{\left\{N3 \to \frac{Mz}{2100},\ N1 \to -\frac{Mz}{2100},\ N4 \to \frac{Mz}{2100},\ N5 \to -\frac{Mz}{2100},\ N2 \to \frac{Mz}{2100},\ N6 \to -\frac{Mz}{2100}\right\}\right\}$$

```
RegPxNew = SolvMatrix /. condPx /. condGeomSym /. L → 200
```

$$\left\{\left\{N3 \to 0,\ N1 \to 0,\ N4 \to -\frac{Px}{2},\ N5 \to -\frac{Px}{2},\ N2 \to 0,\ N6 \to 0\right\}\right\}$$

```
RegPyNew = SolvMatrix /. condPy /. condGeomSym /. L → 200
```

$$\left\{\left\{N3 \to \frac{29\,Py}{84},\ N1 \to -\frac{29\,Py}{84},\ N4 \to \frac{29\,Py}{84},\ N5 \to -\frac{29\,Py}{84},\ N2 \to -\frac{13\,Py}{84},\ N6 \to -\frac{71\,Py}{84}\right\}\right\}$$

```
RegPzNew = SolvMatrix /. condPz /. condGeomSym /. L → 200
```

$$\left\{\left\{N3 \to -\frac{71\,Pz}{84},\ N1 \to -\frac{13\,Pz}{84},\ N4 \to \frac{29\,Pz}{84},\ N5 \to -\frac{29\,Pz}{84},\ N2 \to -\frac{29\,Pz}{84},\ N6 \to \frac{29\,Pz}{84}\right\}\right\}$$

```
RegMxNew = SolvMatrix /. condMx /. condGeomSym /. L → 200
```

$$\left\{\left\{N3 \to -\frac{Mx}{2100},\ N1 \to \frac{Mx}{2100},\ N4 \to -\frac{Mx}{2100},\ N5 \to \frac{Mx}{2100},\ N2 \to \frac{Mx}{2100},\ N6 \to -\frac{Mx}{2100}\right\}\right\}$$

```
RegMyNew = SolvMatrix /. condMy /. condGeomSym /. L → 200
```

$$\left\{\left\{N3 \to \frac{My}{2100},\ N1 \to -\frac{My}{2100},\ N4 \to -\frac{My}{2100},\ N5 \to \frac{My}{2100},\ N2 \to \frac{My}{2100},\ N6 \to -\frac{My}{2100}\right\}\right\}$$

```
RegMzNew = SolvMatrix /. condMz /. condGeomSym /. L → 200
```

$$\left\{\left\{N3 \to \frac{Mz}{2100},\ N1 \to -\frac{Mz}{2100},\ N4 \to \frac{Mz}{2100},\ N5 \to -\frac{Mz}{2100},\ N2 \to \frac{Mz}{2100},\ N6 \to -\frac{Mz}{2100}\right\}\right\}$$

Appendix 2. Bode plots of the forces and torques acts on the pattern relative to spring forces.

Px

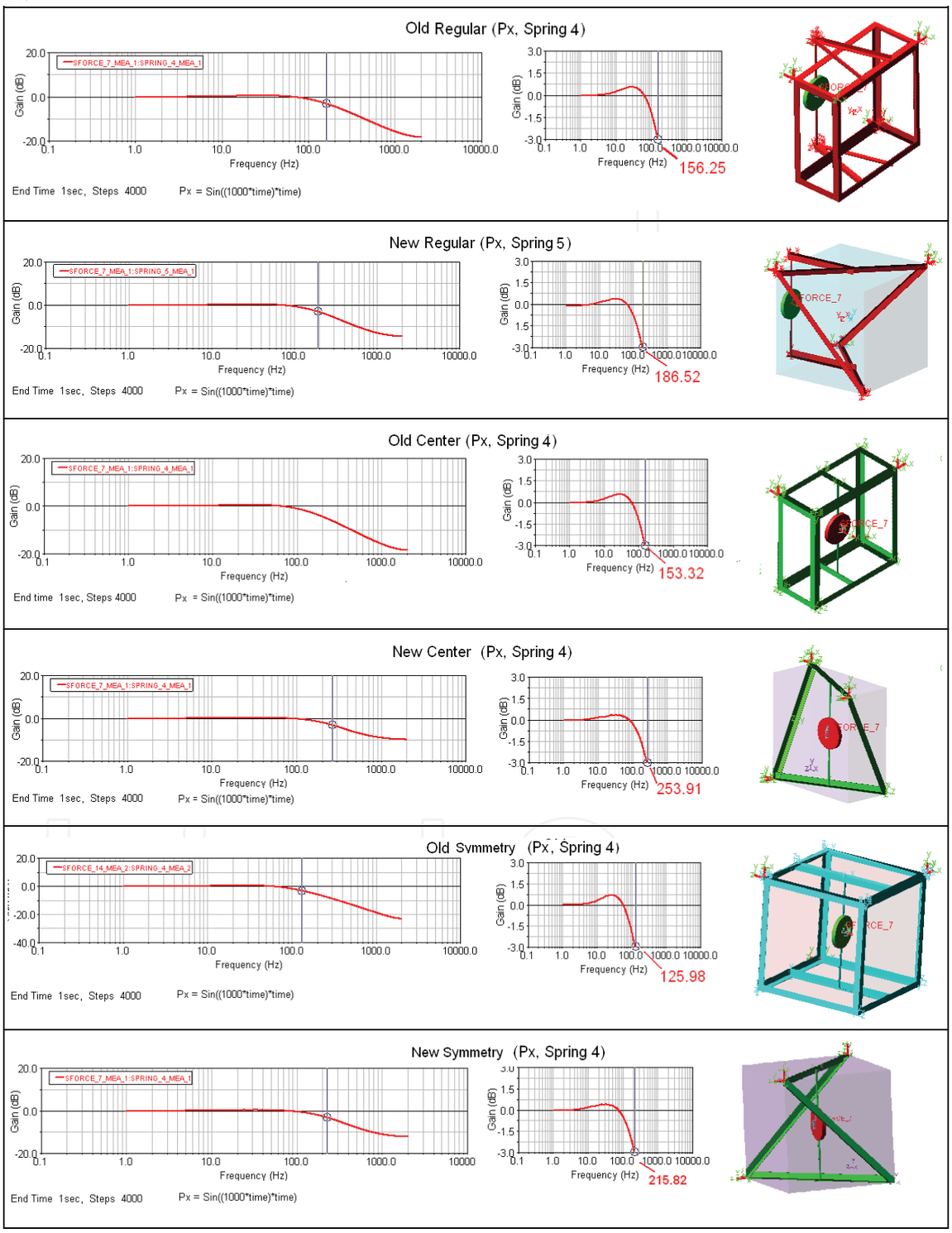

Py

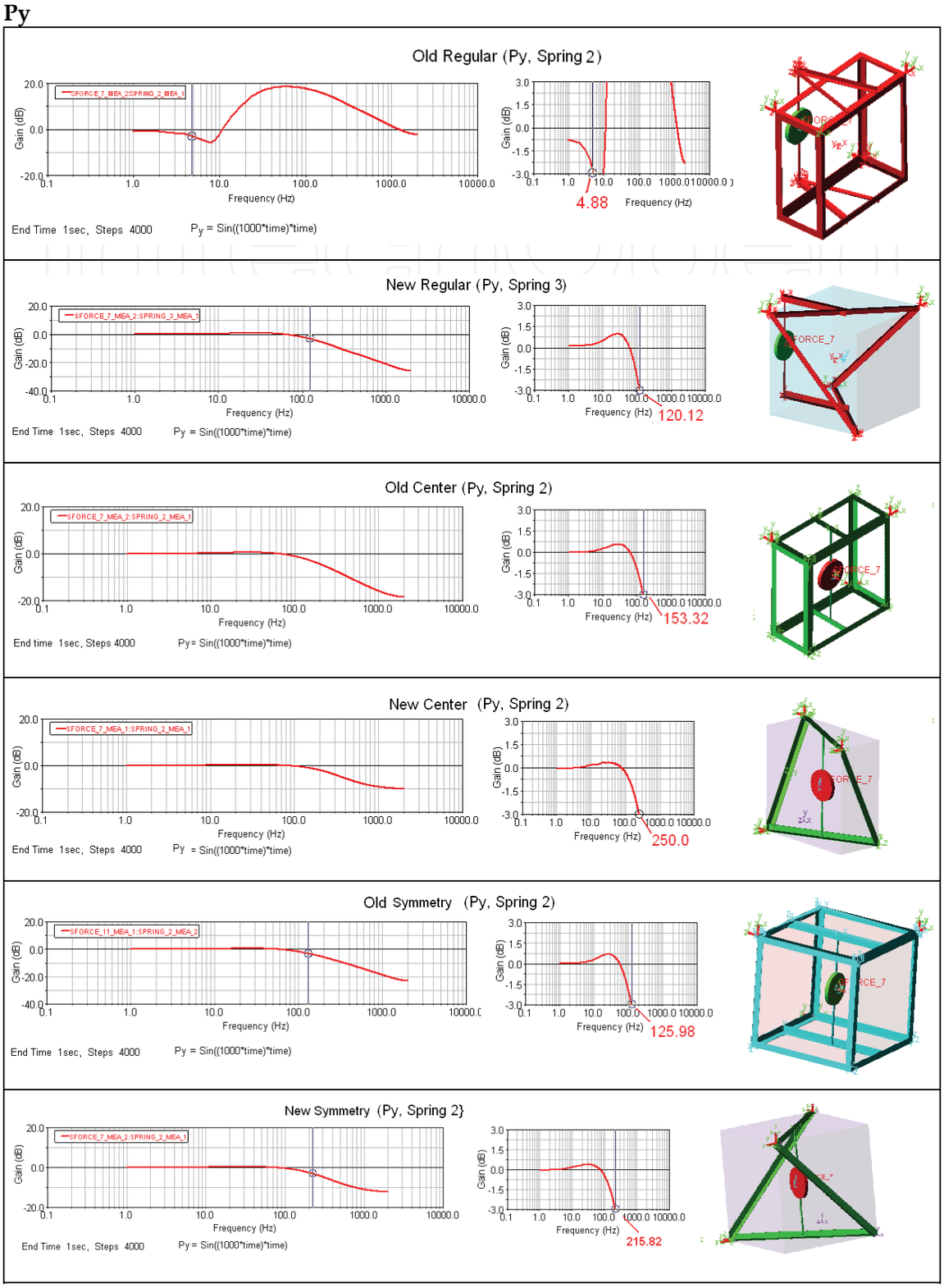
Old Regular (Py, Spring 2)
Gain (dB)
Frequency (Hz)
4.88
End Time 1sec, Steps 4000
Py = Sin((1000*time)*time)
New Regular (Py, Spring 3)
120.12
Old Center (Py, Spring 2)
153.32
End time 1sec, Steps 4000
New Center (Py, Spring 2)
250.0
Old Symmetry (Py, Spring 2)
125.98
New Symmetry (Py, Spring 2)
215.82

Pz

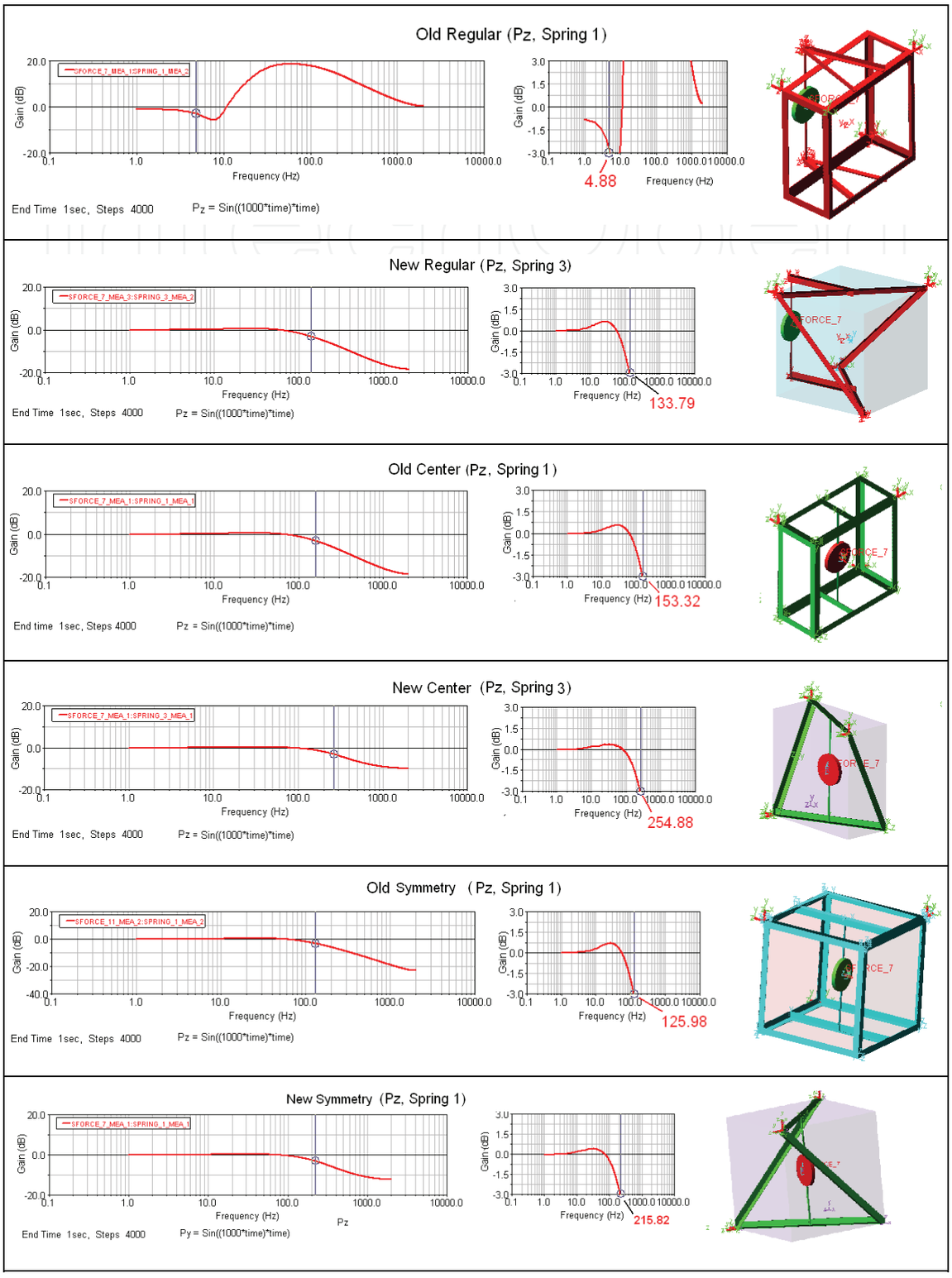
Old Regular (Pz, Spring 1)
Gain (dB)
Frequency (Hz)
4.88
End Time 1sec, Steps 4000
Pz = Sin((1000*time)*time)
New Regular (Pz, Spring 3)
133.79
Old Center (Pz, Spring 1)
153.32
New Center (Pz, Spring 3)
254.88
Old Symmetry (Pz, Spring 1)
125.98
New Symmetry (Pz, Spring 1)
215.82
Pz

Mx

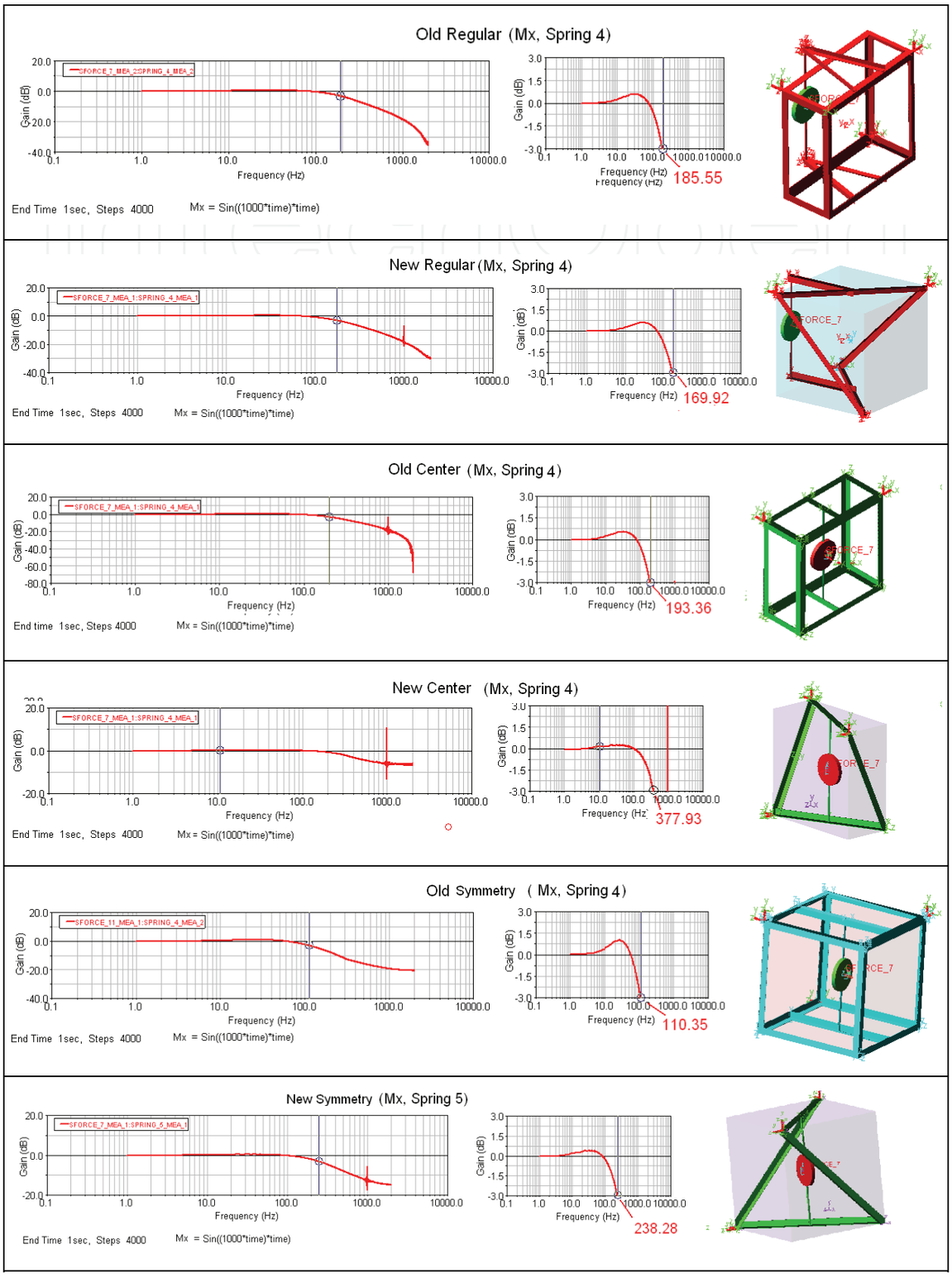
Old Regular (Mx, Spring 4)
SFORCE_7_MEA_2:SPRING_4_MEA_2
Gain (dB)
Frequency (Hz)
185.55
End Time 1sec, Steps 4000
Mx = Sin((1000*time)*time)
New Regular (Mx, Spring 4)
SFORCE_7_MEA_1:SPRING_4_MEA_1
169.92
Old Center (Mx, Spring 4)
193.36
End time 1sec, Steps 4000
New Center (Mx, Spring 4)
377.93
Old Symmetry (Mx, Spring 4)
SFORCE_11_MEA_1:SPRING_4_MEA_2
110.35
New Symmetry (Mx, Spring 5)
SFORCE_7_MEA_1:SPRING_5_MEA_1
238.28

My

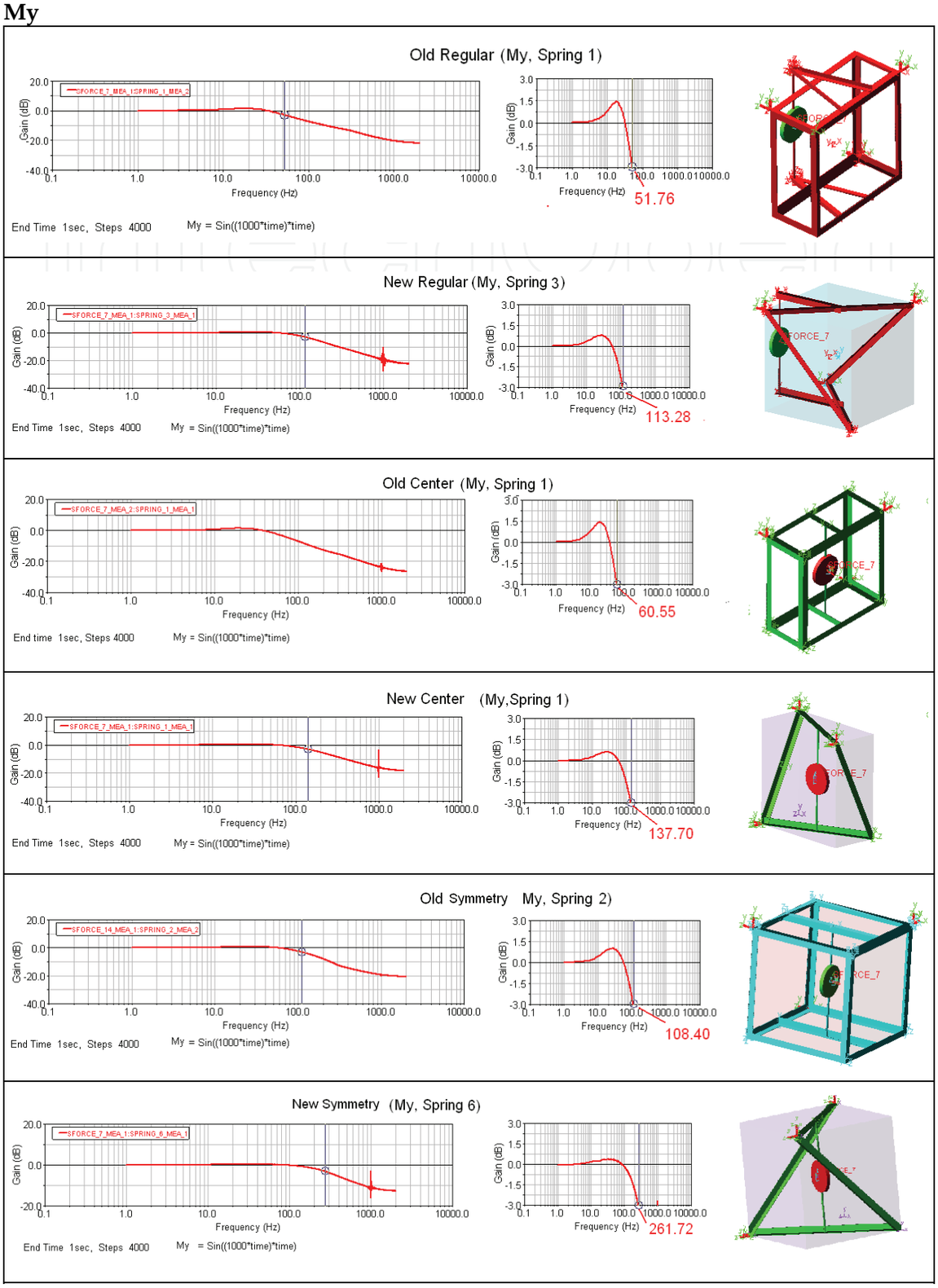
Old Regular (My, Spring 1)
SFORCE_7_MEA_1:SPRING_1_MEA_2
Gain (dB)
Frequency (Hz)
51.76
End Time 1sec, Steps 4000
My = Sin((1000*time)*time)
New Regular (My, Spring 3)
SFORCE_7_MEA_1:SPRING_3_MEA_1
113.28
Old Center (My, Spring 1)
SFORCE_7_MEA_2:SPRING_1_MEA_1
60.55
End time 1sec, Steps 4000
New Center (My,Spring 1)
SFORCE_7_MEA_1:SPRING_1_MEA_1
137.70
Old Symmetry My, Spring 2)
SFORCE_14_MEA_1:SPRING_2_MEA_2
108.40
New Symmetry (My, Spring 6)
SFORCE_7_MEA_1:SPRING_6_MEA_1
261.72

Mz

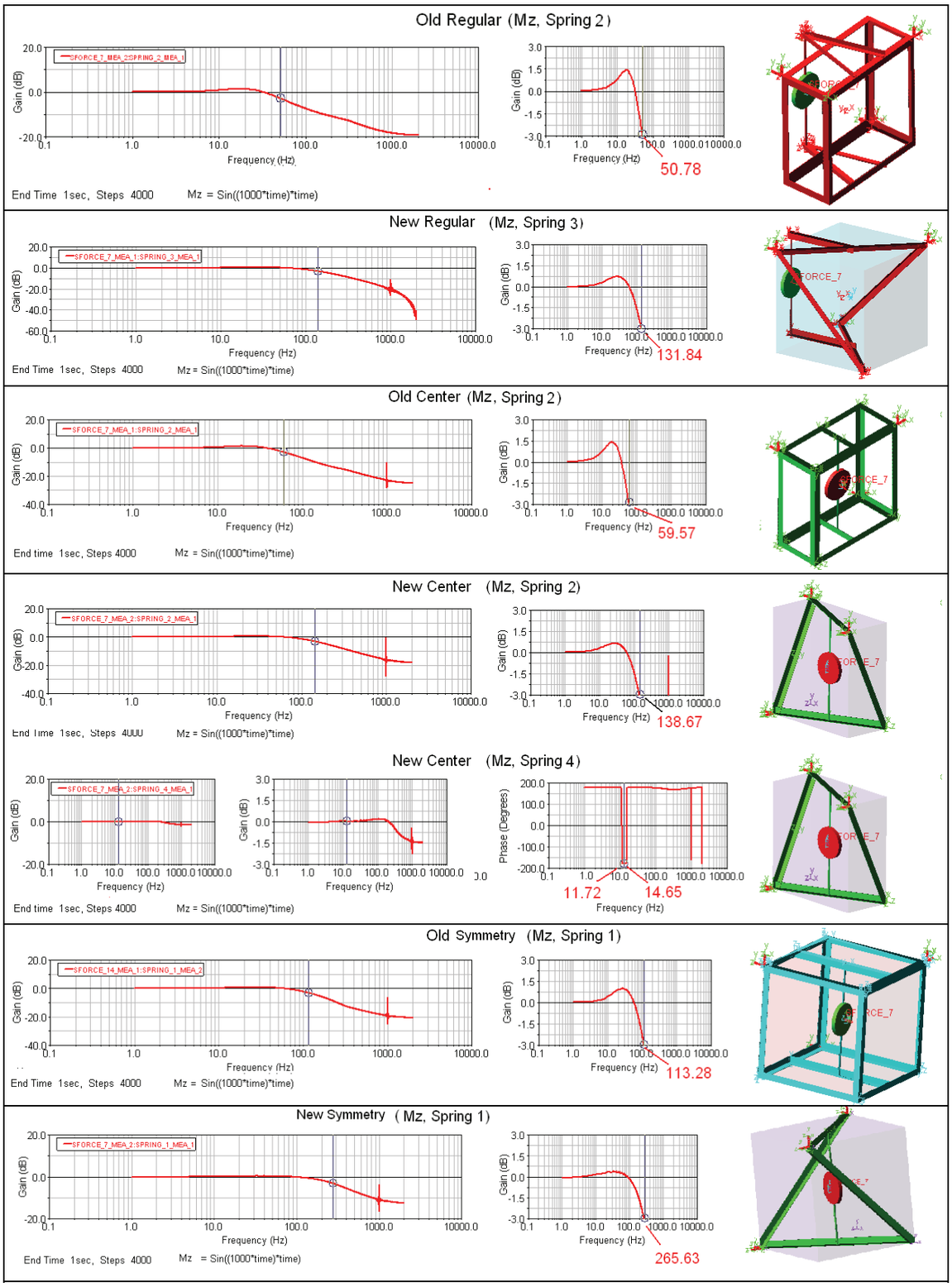
Old Regular (Mz, Spring 2)
Gain (dB)
Frequency (Hz)
50.78
End Time 1sec, Steps 4000
Mz = Sin((1000*time)*time)
New Regular (Mz, Spring 3)
131.84
End Time 1sec, Steps 4000
Mz = Sin((1000*time)*time)
Old Center (Mz, Spring 2)
59.57
End time 1sec, Steps 4000
Mz = Sin((1000*time)*time)
New Center (Mz, Spring 2)
138.67
End Time 1sec, Steps 4000
Mz = Sin((1000*time)*time)
New Center (Mz, Spring 4)
Phase (Degrees)
11.72
14.65
End time 1sec, Steps 4000
Mz = Sin((1000*time)*time)
Old Symmetry (Mz, Spring 1)
113.28
End Time 1sec, Steps 4000
Mz = Sin((1000*time)*time)
New Symmetry (Mz, Spring 1)
265.63
End Time 1sec, Steps 4000
Mz = Sin((1000*time)*time)

Wind Tunnels

Edited by Prof. Satoru Okamoto

ISBN 978-953-307-295-1
Hard cover, 136 pages
Publisher InTech
Published online 10, February, 2011
Published in print edition February, 2011

Although great advances in computational methods have been made in recent years, wind tunnel tests remain essential for obtaining the full range of data required to guide detailed design decisions for various practical engineering problems. This book collects original and innovative research studies on recent applications in wind tunnel tests, exhibiting various investigation directions and providing a birdâ€™s eye view on this broad subject area. It is composed of seven chapters that have been grouped in two major parts. The first part of the book (chapters 1â€“4) deals with wind tunnel technologies and devices. The second part (chapters 5â€“7) deals with the latest applications of wind tunnel testing. The text is addressed not only to researchers but also to professional engineers, engineering lecturers, and students seeking to gain better understanding of the current status of wind tunnels.ã€€Through its seven chapters, the reader will have an access to a wide range of works related to wind tunnel testing.

How to reference

In order to correctly reference this scholarly work, feel free to copy and paste the following:

V. Portman, B. Sandler and V. Chapsky (2011). Dynamically Improved 6-DOF System for Measurements of Forces and Torques in Wind Tunnels, Wind Tunnels, Prof. Satoru Okamoto (Ed.), ISBN: 978-953-307-295-1, InTech, Available from: http://www.intechopen.com/books/wind-tunnels/dynamically-improved-6-dof-system-for-measurements-of-forces-and-torques-in-wind-tunnels

INTECH
open science | open minds

InTech Europe
University Campus STeP Ri
Slavka Krautzeka 83/A
51000 Rijeka, Croatia
Phone: +385 (51) 770 447
Fax: +385 (51) 686 166
www.intechopen.com

InTech China
Unit 405, Office Block, Hotel Equatorial Shanghai
No.65, Yan An Road (West), Shanghai, 200040, China
中国上海市延安西路65号上海国际贵都大饭店办公楼405单元
Phone: +86-21-62489820
Fax: +86-21-62489821

© 2011 The Author(s). Licensee IntechOpen. This chapter is distributed under the terms of the Creative Commons Attribution-NonCommercial-ShareAlike-3.0 License, which permits use, distribution and reproduction for non-commercial purposes, provided the original is properly cited and derivative works building on this content are distributed under the same license.